HL-LHC: PARAMETER SPACE, CONSTRAINTS & POSSIBLE OPTIONS

F. Zimmermann

CERN, Geneva, Switzerland

Abstract

This paper reviews the most promising ingredients to boost the LHC integrated luminosity, including smaller beta*, higher beam intensity, crab crossing, long-range beam-beam compensation, large Piwinski angle, flat longitudinal profile, and variations of bunch length, transverse emittance, crossing angle, and bunch spacing. It discusses how various ingredients conspire or compete, and how they pose different requirements on new LHC hardware and on the beams from the injectors, as well as their relative importance. Special emphasis is given to luminosity-levelling schemes. Finally a proposed roadmap towards HL-LHC and branching points in the research for a solution are sketched.

In particular, this paper points out that raising the beam current is important for reaching a high integrated luminosity, and that long-range beam-beam compensation should be pushed as a simple tool to boost HL-LHC luminosity performance.

INTRODUCTION

The parameter space and ingredients for an LHC luminosity upgrade have first been explored in the 2001 LHC upgrade feasibility study [1]. Later they have been refined and revisited in the frame of CARE-HHH [2], through several targeted workshops, e.g. [3.4,5,6], and, more recently, within the EuCARD-AccNet activity [7]. A review of HL-LHC parameters was presented at the 2010 Chamonix workshop [8]. The key result from Ref. [8] is reproduced in Fig. 1.

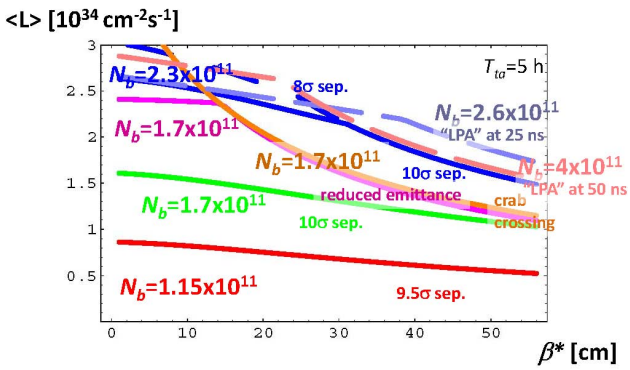

Figure 1: Average luminosity as a function of β^* for the nominal LHC and for various upgrade scenarios with 25-ns and (one with) 50-ns bunch spacing, with a long-range beam-beam separation of at least 8-10σ [8]. An average turnaround time of 5 h, a nominal normalized transverse rms emittance of 3.75 μm, and a maximum total beam-beam tune shift of 0.01 are assumed.

A number of changes have occurred since Chamonix 2010: (1) In the first year of LHC operation the head-on beam-beam limit has been found to be at least a factor of two larger than previously assumed, e.g. to correspond to a total tune shift of 0.02 or higher instead of 0.01 [9]. Though this observation still needs to be confirmed in the presence of the full number of nominal long-range collisions, the larger value of 0.02 will be taken as a new upper bound in our parameter optimization. (2) The LHC operational experience so far indicates the possibility to operate with up to two times lower emittance than nominal, or with twice the nominal beam brightness [9], at least for bunch-spacing values larger than the nominal value of 25 ns. (3) It has been defined that the HL-LHC will employ levelling techniques and run at a constant luminosity of $5\text{x}10^{34}$ $\text{cm}^{-2}\text{s}^{-1}$ [10]. (4) A novel "Achromatic Telescopic Squeezing" (ATS) scheme, entailing beta-beat waves in the arcs [11-12], is a proposal, based on an effective construction and analysis of the corresponding optics [13], to achieve HL-LHC interaction-point (IP) beta functions of less than 30 cm, down to 7.5 cm. In particular, this proposal includes a so-called "flat" optics, with a beta* aspect ratio different from 1 [11-13]. Relevant chromatic aberrations are corrected, respecting the available sextupole strengths in the LHC arcs. The ATS scheme is able to match peak beta function of the order of up to 42 km reached in the triplet (for beta*=7.5cm) to a non-nominal, but regular optics in the adjacent arcs within the strength limits of the matching quadrupoles of the high luminosity insertions [11-12].

This paper is structured as follows. In the first part we discuss schemes for luminosity levelling and introduce the notion of "virtual peak luminosity". Next, the assumptions for estimating annual integrated luminosities are described. It is then shown which combinations of IP beta functions, transverse emittance, beam intensity and bunch spacing are required to reach a given integrated luminosity goal of e.g. 300 fb^{-1} per year. In the following we survey various ingredients for improving the geometric collision spot size, like crab cavities, long-range beam-beam compensators, a higher-harmonic RF system, or unequal "flat" IP beta functions, and we recall the maximal beam intensity available from the injectors (for various stages of the planned injector upgrades) as well as intensity limits in the LHC itself. At this point we are in a position to assemble the results in order to construct a number of HL-LHC parameter sets which could deliver 300 fb^{-1} per year, with varying values of β*, emittance, and bunch spacing, and to determine the beam

intensity required for each of these scenarios. Finally, we draw some conclusions and, based on the earlier findings, we propose a roadmap, milestones, and branching points on the path towards the HL-LHC.

LUMINOSITY LEVELLING

The term "luminosity levelling" refers to intentionally decreasing the peak luminosity and running at approximately constant luminosity during the store. There are several motivations for such operating mode: it reduces the peak event pile up in the particle-physics detectors; it decreases the peak interaction-region (IR) power deposition; and it can maximize the integrated luminosity by potentially lowering the peak value of the beam-beam tune shift.

Around 1998, various luminosity levelling schemes including continuous beta* reduction were considered for the Tevatron Run II [14]. In 2000, luminosity levelling via beta* variation was mentioned for the LHC ion-collision programme ("e.g. squeeze of the beta function during the fill") [15]. Levelling for *pp* collisions in the context of the LHC luminosity upgrade was first proposed in 2007 [16]. Here, levelling with beta* variation or through changes of the bunch length and, thereby, of the Piwinski angle were considered for the so-called "Large Piwinski Angle" (LPA) upgrade scheme. LHC luminosity levelling by crossing-angle variation was proposed a few months later, for the alternative "Early Separation Scheme" of the LHC upgrade [17]. Soon thereafter, luminosity levelling with the crab-cavity RF voltage was suggested for the "Full Crab Crossing" upgrade scheme [18].

For a given levelled luminosity, L_{lev}, the "effective beam lifetime," τ_{eff}, scales with the total beam current. The effective beam lifetime is defined, and computed, by the following two equations,

$$\frac{dN_{tot}}{dt} = -\frac{N_{tot}}{\tau_{eff}} = -n_{IP}\sigma L_{lev},$$

which yield

$$\tau_{eff} = \frac{N_{tot}}{n_{IP}\sigma_{tot}L_{lev}},$$

where n_{IP} denotes the total number of high-luminosity interaction points (IPs), with n_{IP}=2 for the LHC, and σ_{tot} the total cross section. For the LHC centre-of-mass energy the σ_{tot} is quite well known from cosmic-ray experiments to be about 100 mbarn [19].

Figure 2 shows the effective lifetime as a function of total proton intensity for the given HL-LHC target value of levelled luminosity. It is evident that, to obtain a decent proton beam lifetime at the HL-LHC target luminosity, proton intensities above nominal will be required.

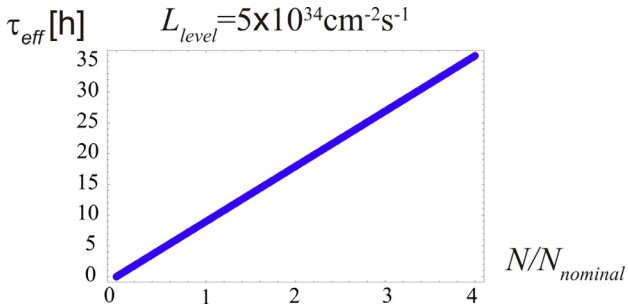

Figure 2: Effective beam lifetime at L_{lev}=5x10^{34} cm^{-2}s^{-1} as a function of total proton intensity in units of nominal intensity (2808 bunches of 1.15x10^{11} protons each).

The general luminosity formula is

$$L = \frac{f_{rev}n_b N_b^2}{4\pi\beta^*\varepsilon} F\left(\phi_{piw}, \Delta x, \ldots\right) \qquad (1)$$

where F denotes a geometric reduction factor from crossing angle and/or beam-beam offset or hourglass effect.

For the luminosity with levelling we can write

$$L_{lev} = f_{lev}(t) L_{\max}(t)$$

where f_{lev} designates a time-dependent levelling factor, $f_{lev} \leq 1$, which characterizes the amount of "levelling detuning" with respect to the unlevelled maximum luminosity that would be possible at this point in time.

We define a "virtual peak luminosity" as

$$\hat{L} \equiv L_{\max}(0)$$
$$= \frac{f_{rev}n_b N_b^2(0)}{4\pi\beta^*(0)\varepsilon} F\left(\phi_{piw,\min}(0)\right)$$
$$= \frac{L_{lev}}{f_{lev}(0)}$$

It is equal to the levelled luminosity divided by the initial value of the levelling detuning factor. In a similar spirit we introduce a virtual peak tune shift.

Various levelling schemes can be considered for the HL-LHC:

(1) Varying the beam-beam offset Δx (successfully applied during LHC operation in 2010 [20]) , which gives rise to the following expressions

$$L_{lev} = \hat{L}\exp\left(-\left(\frac{\Delta x}{2\sigma^*}\right)^2\right);$$

$$\Delta Q_{lev} = \Delta\hat{Q}\,2\left(\left[\exp\left(-\frac{(\Delta x)^2}{2\sigma^{*2}}\right)-1\right]\frac{\sigma^{*2}}{(\Delta x)^2} + \exp\left(-\frac{(\Delta x)^2}{2\sigma^{*2}}\right)\right)$$

where for the tune shift we have assumed an alternating, horizontal and vertical offset at two collision points.

(2) Varying the Piwinski angle ϕ_{piw} ,that is σ_z, θ_c, or V_{crab}. The characteristic equations for this case are

$$L_{lev} \approx \hat{L}\frac{1}{\sqrt{1+\phi_{piw}^2}};$$

$$\Delta Q_{lev} \approx \Delta\hat{Q}\frac{1}{\sqrt{1+\phi_{piw}^2}}$$

where we have assumed two IPs with alternating crossing. (3) Varying the IP beta function β* e.g. at constant ϕ_{piw}, leading to (for round beams):

$$L_{lev} \approx \hat{L}\frac{\hat{\beta}^*}{\beta^*_{lev}};$$

$$\Delta Q_{lev} \approx \Delta\hat{Q}.$$

A few typical time evolutions for these three levelling schemes may serve as an illustration.

First, we consider levelling with the offset Δx. We take the example of L_{peak}=1.0 (or 1.5) x10^{35} cm^{-2}s^{-1}, which means that the initial offset has to be chosen as Δx =1.7 (or 2.1) σ* to get L_{lev}=5x10^{34} cm^{-2}s^{-1}. Figure 3 depicts the subsequent change of Δx as a function of time required to maintain a constant luminosity. Figure 4 shows the resulting evolution of the beam-beam tune shift. The maximum levelling time is 0.3 (or 0.42) τ_{eff} . It is interesting to observe in Fig. 4 that, with offset levelling, the tune shift changes sign during the store.

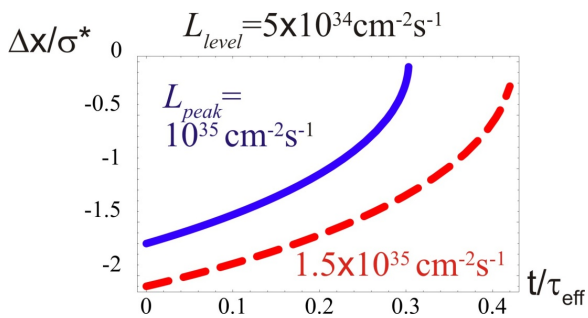

Figure 3: Transverse offset as a function of time in units of the effective beam lifetime, when levelling by offset variation, for two different values of the virtual peak luminosity (as indicated).

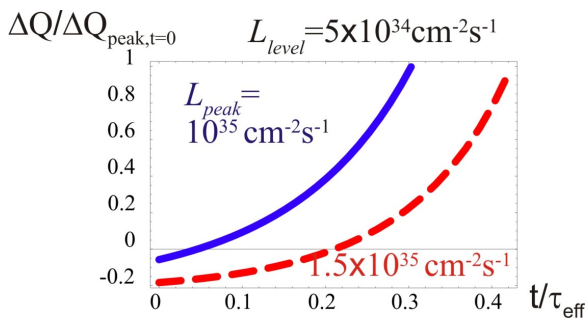

Figure 4: Total beam-beam tune shift in units of the virtual peak tune shift as a function of time in units of the effective beam lifetime, when levelling by offset variation, for two different values of the virtual peak luminosity (as indicated).

Second, we look at levelling with θ_c or V_{crab}. We take the same example values for the virtual peak luminosity as before, that is L_{peak}=1.0 (or 1.5) x10^{35} cm^{-2}s^{-1} . In this case the initial Piwinski angle has to be set to ϕ_{piw}=1.7 (or 2.8) rad in order to obtain L_{lev}=5x10^{34} cm^{-2}s^{-1}. Figure 5 shows the change of ϕ_{piw} as a function of time needed in order to keep a constant luminosity. Figure 6 displays the implied evolution of the beam-beam tune shift for levelling with the Piwinski angle. The maximum levelling time is 0.3 (0.42) τ_{eff} as before. Figure 6 indicates that when levelling with the Piwinski angle, the beam-beam tune shift increases during the store, which might not always be desirable.

Third, we discuss levelling with β^*. Proceeding as before, we find that with a virtual peak luminosity of L_{peak}=1.0 (or 1.5) x10^{35} cm^{-2}s^{-1} at β*=0.15 m, we need to increase the initial IP beta function to β*=0.3 (or 0.45) m in order to get L_{lev}=5x10^{34} cm^{-2}s^{-1}. Figure 7 illustrates the evolution of β* as a function of time for constant luminosity, and Fig. 6 the evolution of the beam-beam tune shift with β* levelling. When levelling by reducing β*, the tune shift decreases during the store (see Fig. 8). The maximum levelling time is again 0.3 (0.42) τ_{eff} , which is hence independent of the levelling scheme, and only depends on the value of the virtual peak luminosity and on the target levelling luminosity.

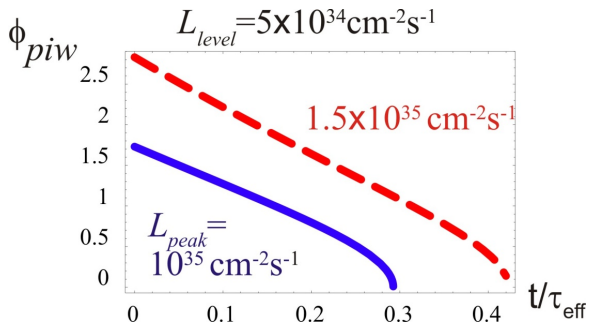

Figure 5: Piwinski angle as a function of time in units of the effective beam lifetime, when levelling by varying the Piwinski angle, for two different values of the virtual peak luminosity (as indicated).

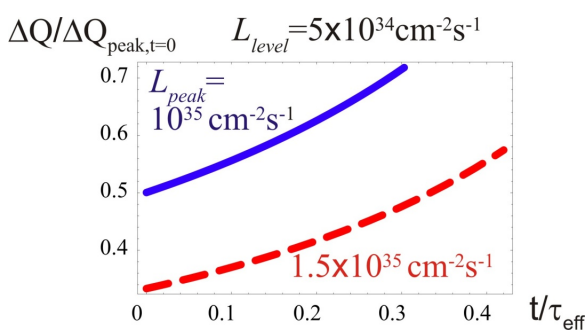

Figure 6: Total beam-beam tune shift in units of the virtual peak tune shift as a function of time in units of the effective beam lifetime, when levelling by varying the Piwinski angle, for two different values of the virtual peak luminosity (as indicated).

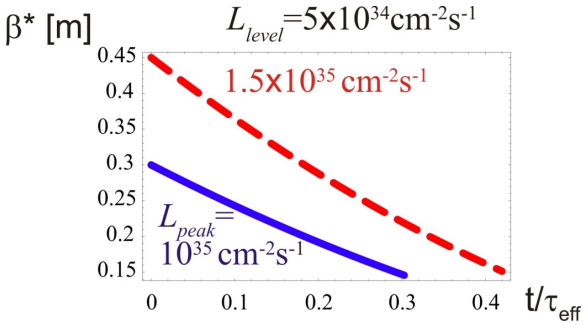

Figure 7: IP beta function as a function of time in units of the effective beam lifetime, when levelling by varying β^*, for two different values of the virtual peak luminosity (as indicated).

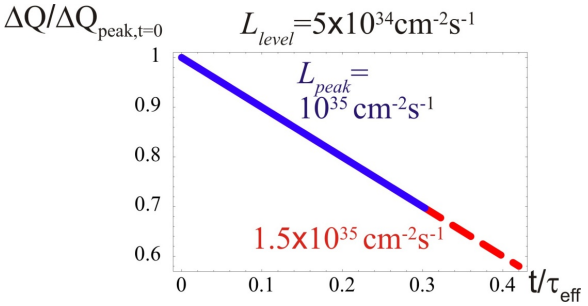

Figure 8: Total beam-beam tune shift in units of the virtual peak tune shift as a function of time in units of the effective beam lifetime, when levelling by β^* variation, for two different values of the virtual peak luminosity (as indicated).

For a given levelled luminosity, the maximum levelling time in units of τ_{eff} is a function of the virtual peak luminosity according to

$$\frac{t_{lev}}{\tau_{eff}} = 1 - \sqrt{\frac{L_{lev}}{\hat{L}_{peak}}} \ ,$$

which is shown in Fig. 9.

The absolute levelling time t_{lev} also depends on the beam intensity. Figure 10 shows the absolute levelling time as a function of the virtual peak luminosity for two different proton beam intensities. The absolute levelling time scales linearly with the total beam intensity.

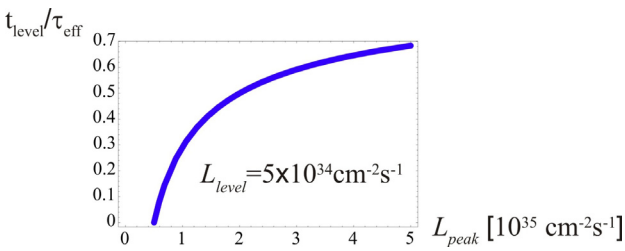

Figure 9: Maximum levelling time in units of effective beam lifetime as a function of the virtual peak luminosity. The curve is independent of the levelling scheme.

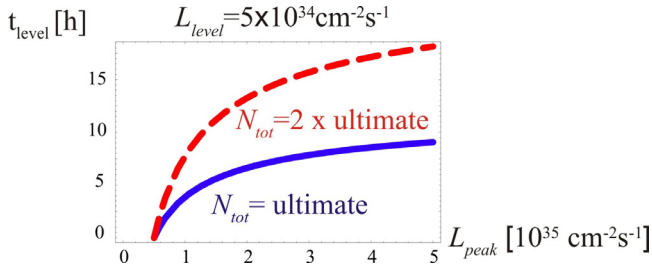

Figure 10: Maximum levelling time in units of hours as a function of the virtual peak luminosity, for two different proton beam intensities.

For estimating integrated luminosity at the HL-LHC, we make the following assumptions:

- two high-luminosity collision points;
- beam & luminosity lifetime are dominated by *p* consumption;
- 200 physics days of proton run per year (w/o restart, w/o TS's, w/o MD periods);
- 5 h turnaround time from physics to physics;
- 75% machine availability.

The last number appears conservative. In November 2010 the LHC availability has already reached 80% [21]. Many other accelerator and/or collider projects around the world have obtained higher availability numbers; see Table 1.

Table 1: Machine availability for various accelerators.

PEP-II [22]	87%
LCLS [22]	94%
Tevatron (best) [23]	97.5%
RHIC (2010-11 run) [24]	82%
LHC Nov. 2010 [21]	80%

We can then calculate the integrated luminosity with levelling at 5x10³⁴ cm⁻²s⁻¹. It depends only on the virtual peak luminosity and on the total beam current, as is illustrated in Fig. 11.

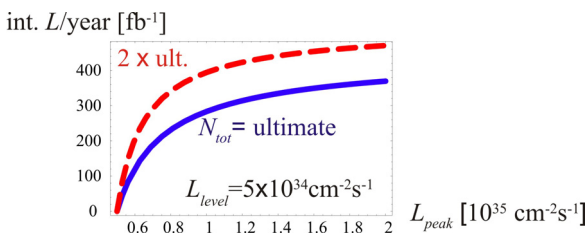

Figure 11: Annual luminosity as a function of virtual peak luminosity for two different total proton-beam intensities.

For example, getting 300 fb^{-1} per year, at ultimate intensity requires a virtual peak luminosity of L_{peak}=1.10x10^{35} cm^{-2}s^{-1}, while at two times the ultimate intensity a peak luminosity of L_{peak}=0.71x10^{35}cm^{-2}s^{-1} would be needed (and with higher beam current it would also be much easier to get this virtual peak luminosity).

As shown in Fig. 12, we can "invert" the above relation and compute the beam intensity required to obtain a given

target annual luminosity as a function of the virtual peak luminosity.

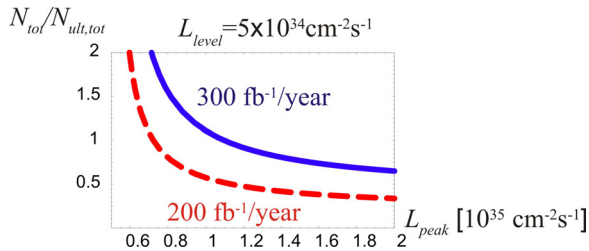

Figure 12: Total beam intensity required to reach 300 fb^{-1} or 200 fb^{-1} per year, as a function of the virtual peak luminosity.

We note that for a given bunch spacing the virtual peak luminosity on the horizontal axis of Fig. 12 scales with the square of the beam intensity, so that the beam intensity enters linearly in vertical direction and quadratically towards the right. This underlines the tremendous importance of beam intensity for reaching the HL-LHC integrated luminosity target.

How much do we need to squeeze or what is the benefit of squeezing further? To answer this question, it is straightforward to factor out the intensity from the peak luminosity and to convert Fig. 12 into a curve of geometric beam size reduction as a function of beam intensity. The result is shown in Fig. 13.

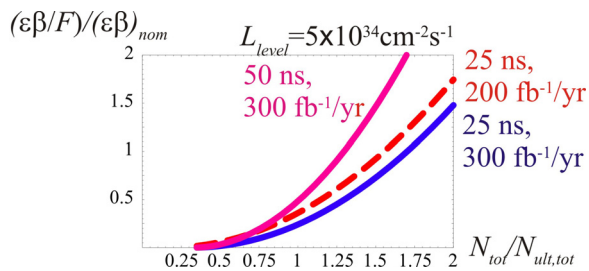

Figure 13: Geometric beam-size reduction $\beta^*\varepsilon/F$ (see Eq. (1)) needed to meet the annual integrated luminosity goal, including crossing-angle effect and normalized to the nominal value of ($\beta^*\varepsilon$), as a function of the total proton beam intensity, for two different values of bunch spacing and luminosity target.

For example, to obtain 300 fb^{-1} per year at N_b=2x10^{11} bunch population and 25 ns spacing we need to reduce ($\beta^*\varepsilon$)/F by a factor 0.38 compared with the nominal ($\beta^*\varepsilon$), while at N_b=3.4x10^{11} and 50 ns we need to reduce ($\beta^*\varepsilon$)/F only by a factor 0.48.

Holding the emittance constant, equal to nominal, and assuming a long-range beam-beam separation of 8.5σ (achieved with long-range compensators), Fig. 13 can be converted into a requirement on β^*, presented in Fig. 14.

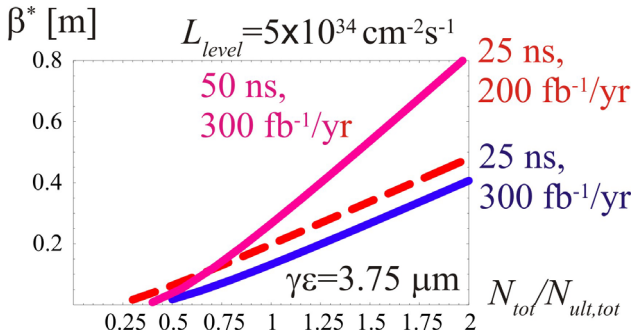

Figure 14: IP beta function needed for delivering 300 or 200 fb^{-1} per year as a function of total proton intensity in units of ultimate intensity, for two different values of bunch spacing, at a constant transverse normalized emittance equal to nominal.

Figure 14 illustrates the trade-off between proton beam intensity and β^*, for a given integrated luminosity goal and bunch spacing. For 25-ns bunch spacing the design β^* value of 55 cm would suffice at twice the ultimate intensity (that is, at 2 x 2808 x 1.7 x 10^{11} protons), while for nominal intensity β^* must be shrunk to below 20 cm. A bunch spacing of 50 ns would allow for two times larger β^* values at the same total intensity.

Instead of varying β^* we can keep it constant, equal to nominal (0.55 m), and reduce the transverse emittance to meet the integrated luminosity goal. The emittance required as a function of total beam intensity is shown in Fig. 15, again for a long-range separation of 8.5σ. With 50-ns spacing the nominal emittance would suffice at about 1.5 times the ultimate intensity

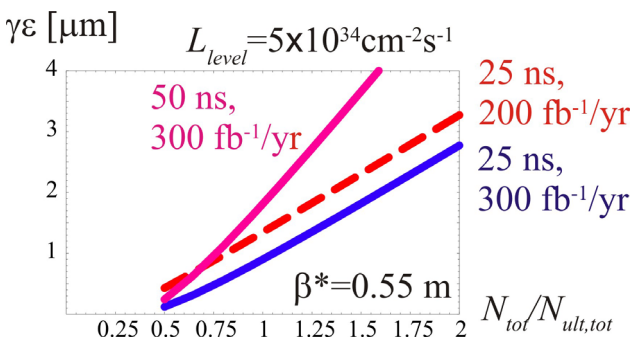

Figure 15: Transverse normalized emittance needed for delivering 300 or 200 fb^{-1} per year as a function of total proton intensity in units of ultimate intensity, for two different values of bunch spacing, at a constant IP beta function equal to nominal.

Table 2 shows (ε,β^*) combinations that would provide the target annual luminosity at a total intensity equal to the ultimate LHC intensity, for two different bunch spacings. As can be seen, the scenarios with 50-ns bunch spacing are particularly attractive and they would allow reaching the target with an IP beta function of about 30

cm and close to nominal emittance, at ultimate total proton intensity.

Table 2: ε–β* combinations that would deliver a target annual luminosity of 300 or 200 fb^{-1} per year at ultimate total proton intensity.

luminosity	spacing	norm. emittance	IP beta
300 fb^{-1}/yr	25 ns	3.75 μm	0.13 m
200 fb^{-1}/yr	25 ns	3.75 μm	0.20 m
300 fb^{-1}/yr	**50 ns**	**3.75 μm**	**0.27 m**
300 fb^{-1}/yr	25 ns	0.90 μm	0.55 m
200 fb^{-1}/yr	25 ns	1.35 μm	0.55 m
300 fb^{-1}/yr	**50 ns**	**1.81μm**	**0.55 m**
300 fb^{-1}/yr	25 ns	1.65 μm	0.30 m
200 fb^{-1}/yr	25 ns	2.47 μm	0.30 m
300 fb^{-1}/yr	**50 ns**	**3.32 μm**	**0.30 m**

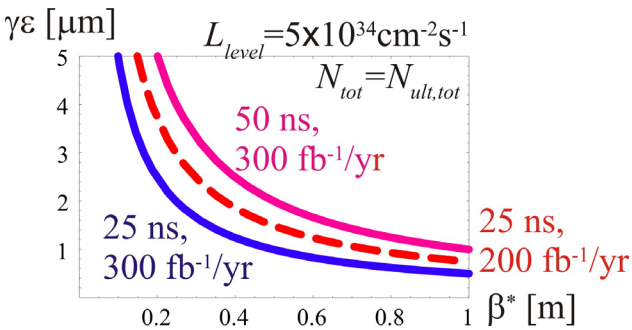

Figure 16: Normalized emittance yielding target integrated luminosity at ultimate proton beam intensity, as a function of IP beta function.

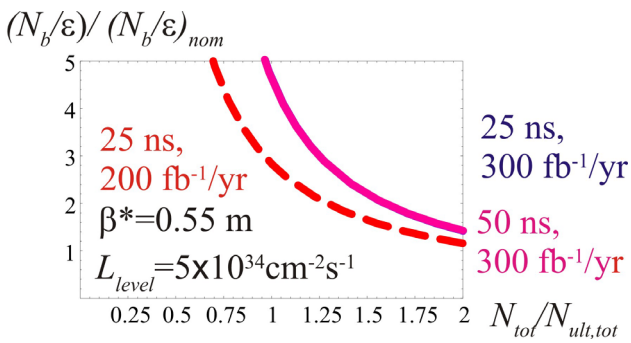

Figure 17: Beam brightness, normalized to ultimate brightness at 25 ns spacing and nominal bunch length, required for delivering 300 or 200 fb^{-1} per year as a function of total proton intensity in units of ultimate intensity, for two different values of bunch spacing, at a constant IP beta function equal to nominal (0.55 m), with emittance varying as in Fig. 16. The curve for 25-ns spacing equals the one for 50-ns spacing.

Figure 16 graphically illustrates the relation between normalized transverse emittance and IP beta function that must be met to reach the target HL-LHC integrated luminosity at ultimate proton beam intensity. Figures 17 and 18 show the bunch brightness as a function of total intensity, corresponding to the emittance variation in Fig. 15 and to the β* variation in Fig. 14, respectively.

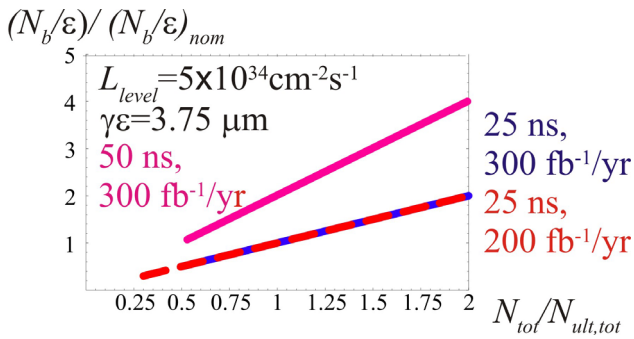

Figure 18: Beam brightness, normalized to ultimate brightness at 25 ns spacing and nominal bunch length, required for delivering 300 or 200 fb^{-1} per year as a function of total proton intensity in units of ultimate intensity, for two different values of bunch spacing, at a constant transverse normalized emittance equal to nominal (3.75 μm), with β* varying as in Fig. 15. At a given bunch spacing and emittance, the curves are independent of the target luminosity.

APPROACHES AND INGREDIENTS TO BOOST LHC LUMINOSITY

Alternative approaches to increase the LHC intensity include the following: (1) low β* & crab cavities (a few tens of MV), (2) low β* & higher harmonic RF (e.g. 7.5 MV at 800 MHz) plus long-range compensation, and (3) operating in a regime of large Piwinski angle together with long-range beam-beam compensation. These three collision schemes are sketched in Fig. 19. Interaction-point β* values below 30 cm could be achieved with the ATS optics [11-13,25]. In all the aforementioned scenarios the beam intensity should be pushed to the "limit" as well.

Each collision scheme could be implemented with either 25-ns or 50-ns bunch spacing, and correspondingly adjusted bunch charge. The value of β* is also a variable. In addition, for each case one can consider both round-beam collisions and collisions with different IP beta functions in the two transverse planes ($\beta_x^* \neq \beta_y^*$), in this case with alternating aspect ratio at the two primary IPs. A large (infinite) number of parameter combinations exist which can meet the target value for the HL-LHC integrated luminosity.

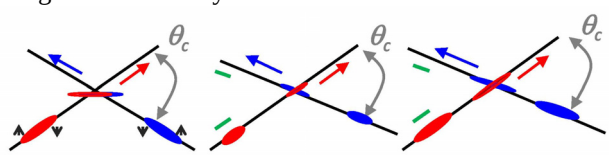

Figure 19: Alternative collisions schemes for the HL-LHC; low β* & crab cavities [left]; low β* & higher harmonic RF plus long-range compensation [center], and collisions at large Piwinski angle together with long-range beam-beam compensation [right].

Crab cavities offer the following benefits: They improve the geometric overlap for small β* and large crossing angle (which is one of the primary motivations for installing them in the LHC); they can potentially boost the beam-beam limit (a potential additional benefit); they allow for an easy and transparent luminosity levelling (another key motivation for the LHC); and they would avoid off-center collisions from beam loading (an additional benefit for the LHC); the beam loading issue was highlighted in [26]. An ATS-type optics solution accommodating crab cavities with $\beta_{x,y}^{*}$=15 cm has been constructed [25].

A number of points need to be addressed prior to a full crab-cavity installation in the LHC, including the emittance growth from crab-cavity RF noise, the effect of the crab-cavity impedance, the size and impact of any field nonlinearity, machine protection issues in case of a crab-cavity failure, trip rate, various technical challenges, and the time line.

There exist 4 to 5 promising designs for compact crab cavities which could be accommodated in the LHC interaction regions (see Fig. 20). The present plan is to perform SPS/LHC prototype beam tests in about 2015/16, before a final decision is taken.

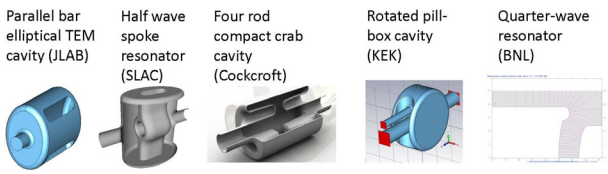

Figure 20: Candidate designs for compact HL-LHC crab cavities presented at the LHC-CC'10 workshop [27]: ODU/JLAB design by J. Delayen; SLAC design by Z. Li et al; CI design by G. Burt; KEK design by K. Nakanishi; and BNL design by I. Ben-Zvi.

A number of recent simulations studies suggest that crab-cavities can raise the LHC beam-beam limit. Figure shows results from a weak-strong beam-beam simulation by D. Shatilov and M. Zobov [28] using the Lifetrac code. A frequency map analysis of tune diffusion in the A_x-A_y normalized amplitude space (extending to 10σ) reveals that the crab crossing suppresses all important resonances which are present in case of a finite crossing angle, as is shown in Fig. 21.

Figure 22 present results from a strong-strong beam-beam simulation by K. Ohmi for a different set of LHC parameters [29], which indicate that the luminosity lifetime with crab crossing is 10 times higher than without.

Long-range beam-beam compensation using "wires" has first been proposed by Jean-Pierre Koutchouk [30]. Prototype beam-beam compensators have been built and deployed for beam studies at the SPS [31] and in RHIC [32]. At present 2x2 water-cooled units are installed in the SPS (two with remote control), and 1x2 spare units are ready for installation. The two RHIC compensators have recently been dismounted to increase the aperture for new Roman pot experiments. They have been donated for SPS and LHC studies. The 1st RHIC compensator is already stored at CERN; the 2nd is being shipped. In total 5 long-range beam-beam compensator sets will soon be available on the CERN site. Different from the SPS design, the RHIC compensators are air-cooled.

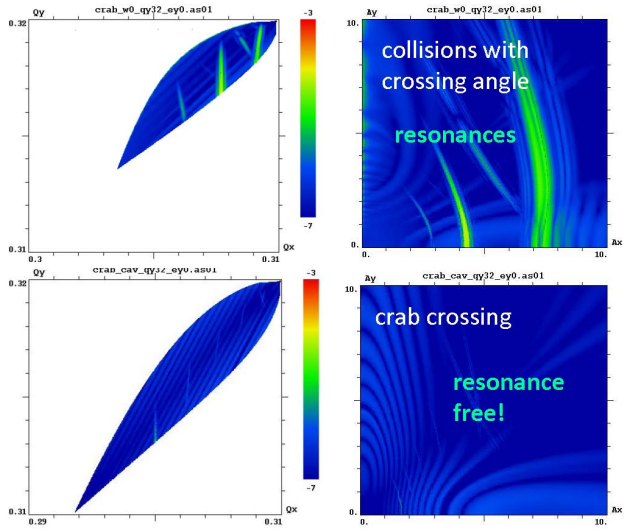

Figure 21: Frequency map analysis of weak-strong beam-beam simulations for LHC scenarios without [top] and with crab crossing [bottom] [28]. The beam parameters assumed were $\varepsilon_{x,y}$ =0.5 nm, E = 7 TeV, β^{*}_{x} = *30* cm, β^{*}_{y} = 7.5 cm, σ_z = 11.8 cm, θ_c= 315 mrad (ϕ_{piw} =1.5), N_b = 4.0x10^{11}, Q_s =0.002, $\Delta Q_{x,y}$ ~ -0.0065, and a single interaction point.

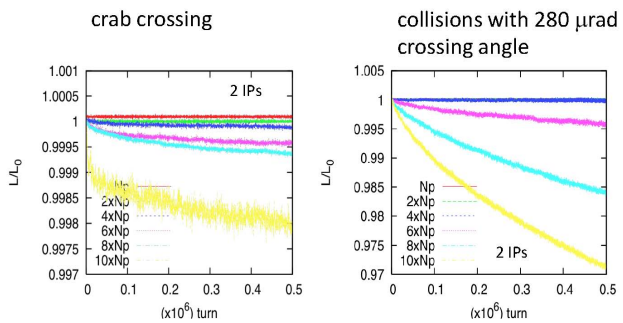

Figure 22: HL-LHC luminosity as a function of time from a strong-strong beam-beam simulation with crab crossing [left] and crossing angle [right] [29]. This simulation was performed for the nominal LHC considering 2 interaction points with alternating crossing, and a crossing angle of 280 μrad. The various curves correspond to different bunch intensities given as multiples of the nominal intensity (color code).

Figure 23 shows a photo of one of the SPS compensators, which is equipped with independent three wires in order to be able to compensate, or mimic, long-range beam-beam collisions in the horizontal plane, in the vertical plane, and at 45 degrees.

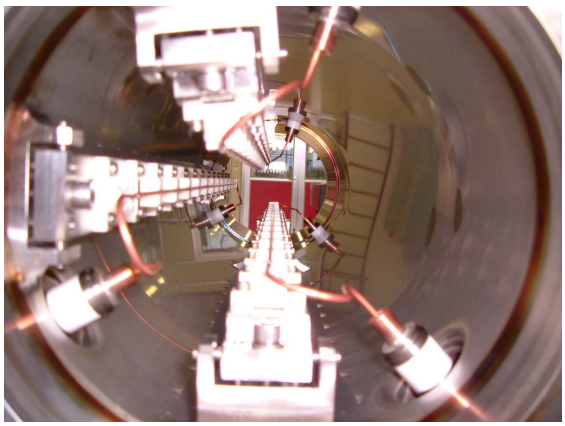

Figure 23: Photograph of a long-range beam-beam compensator prototype unit installed in the CERN SPS, with three independent wires mounted at a horizontal, vertical, and 45-degree separation from the beam (G. Burtin, J.-P. Koutchouk, F. Zimmermann et al.).

Figure 24 illustrates the potential benefit from the long-range beam-beam compensation. Shown is the normalized crossing angle as a function of bunch intensity. Without compensators the minimum norrnalized crossing angle required in the LHC increases as a function of bunch intensity N_b and spacing $T_{\rm sep}$ roughly as [33]

$$\frac{\theta_{c,\min}}{\sigma^{*}} \approx 6 + 3.5\sqrt{\frac{N_b}{1.05\times10^{11}}\,\frac{25\ \text{ns}}{T_{sep}}\,\frac{n_{LR}}{72}}\ ,$$

which is represented by the two sold lines in the figure. Long-range beam-beam compensation would be effective at a separation of about 8.5σ, where the field of the other beam is well approximated by a 1/*r* law up to a betatron amplitudes of about 6σ - the nominal location of the LHC primary collimators.

Specifically, Fig. 24 demonstrates how the long-range compensators enable further increases in beam intensity while maintaining a constant crossing angle corresponding to 8.5 times the rms IP beam divergence, to be compared with a crossing angle of 9.5σ*' for the nominal LHC design.

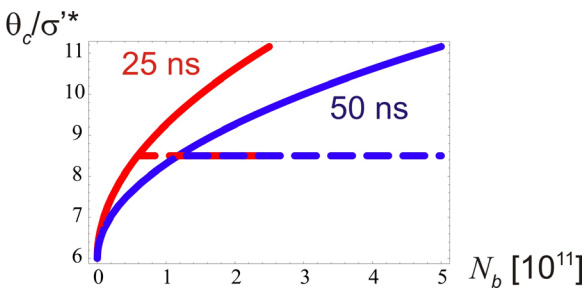

Figure 24: Normalized LHC crossing angle as a function of bunch intensity without (solid) and with long-range compensation (dashed) for 25-ns (red) and 50-ns bunch spacing (blue), according to the above formula.

For the installation of future long-range beam-beam compensators in the LHC 3-m long sections have been reserved at 104.93 m (center position of the wire) on either side of LHC IP1 and IP5, as documented by an LHC engineering change order issued by J.-P. Koutchouk in 2004 (Fig. 25).

If the colliding beams are not round but "**flat**" **with** $\beta_x^* \neq \beta_y^*$, the minimum crossing angle may not only depend on the normalized separation in the plane of crossing, but also on the beta function in the other plane. Considering alternating crossing with $\beta_x^* > \beta_y^*$ and horizontal crossing in one IP, and $\beta_x^* < \beta_y^{**}$ plus vertical crossing in the second IP, and comparing the moduli of the long-range beam-beam tune shift with those for round-beam collisions, we expect that, for flat beam collisions, the minimum separation needed in the plane of crossing for an IP beta function ratio of 4 could be about 50% larger than estimated by looking only at the separation in the plane of crossing, due to the fact that the beta function is larger in the orthogonal plane. The validity of the above reasoning needs to be confirmed in tracking simulations.

Using formulae of [34] for the tune shift induced by a single centered flat-beam collision, and denoting $r=\beta_x^*/\beta_y^*$ (with $\beta_x^* > \beta_y^*$), the total "head-on" flat-beam tune shift with alternating crossing at two collision points is

$$\Delta Q_{tot,\,flat} = \frac{r_p N_b}{2\pi\gamma\varepsilon}\left(\frac{1+\sqrt{\frac{1}{r}\left(1+\phi_{piw}^2\right)}}{\left(1+\phi_{piw}^2\right)+\sqrt{\frac{1}{r}\left(1+\phi_{piw}^2\right)}}\right)$$

where the normalized emittance is assumed to be the same in the two transverse planes, i.e. $\gamma\varepsilon=\gamma\varepsilon_x=\gamma\varepsilon_y$. For r=1 the above reduces to the standard round-beam expression.

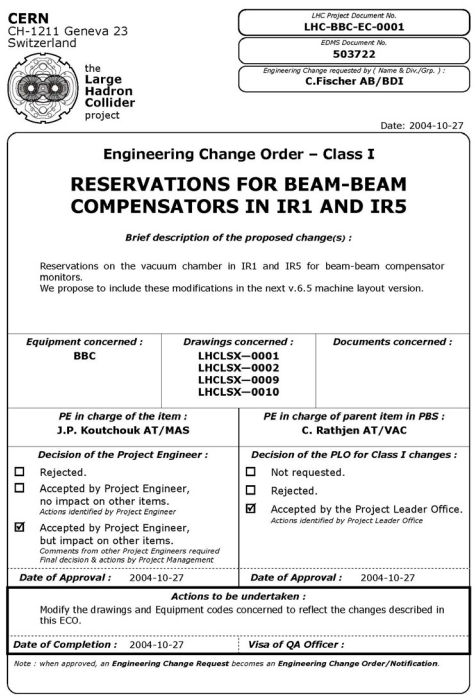

CERN
CH-1211 Geneva 23
Switzerland

the Large Hadron Collider project

LHC Project Document No.: LHC-BBC-EC-0001
EDMS Document No.: 503722
Engineering Change requested by (Name & Div./Grp.) : C.Fischer AB/BDI

Date: 2004-10-27

Engineering Change Order – Class I

RESERVATIONS FOR BEAM-BEAM COMPENSATORS IN IR1 AND IR5

Brief description of the proposed change(s) :

Reservations on the vacuum chamber in IR1 and IR5 for beam-beam compensator monitors.
We propose to include these modifications in the next v.6.5 machine layout version.

Equipment concerned :	*Drawings concerned :*	*Documents concerned :*
BBC	LHCLSX—0001 LHCLSX—0002 LHCLSX—0009 LHCLSX—0010	

PE in charge of the item :	*PE in charge of parent item in PBS :*
J.P. Koutchouk AT/MAS	C. Rathjen AT/VAC

Decision of the Project Engineer :	*Decision of the PLO for Class I changes :*
☐ Rejected.	☐ Not requested.
☐ Accepted by Project Engineer, no impact on other items. *Actions identified by Project Engineer*	☐ Rejected.
☑ Accepted by Project Engineer, but impact on other items. *Comments from other Project Engineers required Final decision & actions by Project Management*	☑ Accepted by the Project Leader Office. *Actions identified by Project Leader Office*
Date of Approval : 2004-10-27	*Date of Approval :* 2004-10-27

Actions to be undertaken :
Modify the drawings and Equipment codes concerned to reflect the changes described in this ECO.

Date of Completion : 2004-10-27 | *Visa of QA Officer :*

Note : when approved, an ***Engineering Change Request*** *becomes an* ***Engineering Change Order/Notification.***

Figure 25: Engineering change order reserving space for long-range beam-beam compensators around LHC IP1 and IP5, dating from the year 2004.

A **higher harmonic RF system** in the LHC, as proposed in [35], could help the HL-LHC performance in a number of ways. It could be used to lengthen or shorten the bunches, or for tailoring the bunch profile (creating longitudinally peaked or flat bunches), and most importantly for increasing Landau damping and enabling higher beam intensity. The higher-harmonic RF system can be thought of as a "Landau octupole" for the longitudinal plane. The report [35] discussed higher-harmonic RF systems at 1.2 GHz and 800 MHz. The presently favored system is at 800 MHz [36]. This system, with a voltage of about 7.5 MV, would raise the stability gain by at least a factor of 3, e.g. allowing for three times higher beam intensity or for lower longitudinal emittance (avoiding the controlled blow up in the LHC) and, thereby, shorter bunches.

MAXIMUM BEAM INTENSITY

The beam intensity available from the injectors increases with the proposed injector upgrades. The projected intensities in various upgrade phases, and for different values of bunch spacing and transverse emittance, are summarized in Table 3, taken from [9]. As we will show later, the last two rows correspond to "HL-LHC" class intensities, i.e. intensities needed to meet the HL-LHC design goals for integrated luminosity. We will argue that it would be helpful if the maximum intensity could still be increased by 10-20% beyond these values.

Table 3: Intensity and emittances available from the LHC injector complex for various upgrade phases.

	spacing [ns]	bunch intensity [10^{11}]	transverse norm. emittance [μm]
nominal	25	1.15	3.75
available "now"	25	1.20	3.75
available "now"	50	1.70	3.75
available "now"	50	1.70	2.50
w LINAC4	25	1.40	3.75
w LINAC4	50	2.50	3.75
w LINAC4+LIU	25	2.00	2.50
w LINAC4+LIU	50	3.30	3.75

An intensity limit in the LHC itself is imposed by the cooling capacity available for the beam screen and magnet cold bore with regard to beam-induced heat loads. The cooling capacity for the cold LHC arcs is limited both globally, by the cooling power of the cryo plants, which must also cool the interaction region quadrupoles – at high luminosity subjected to large heat from collision debris –, and locally, by the hydraulic impedance of the beam-screen cooling loops [37-39]. It is assumed that the HL-LHC will have dedicated cryoplants for the interaction region and the RF system, and that the existing cryoplants are used for the cooling of the LHC arcs only.

In the LHC arcs proper, synchrotron radiation, image currents (together with the resistive wall impedance) and electron cloud are the main sources of heat load. The heat from synchrotron radiation and impedance can be fairly accurately calculated [38,39]. Heat load due to image currents and synchrotron radiation increase with bunch intensity as shown in Figs. 26-28, for three different combinations of bunch length and bunch spacing. The figures demonstrate that the sum of these heat loads always stays below the maximum available local cooling capacity of about 2.3 W/m per aperture. Bunch intensities up to $2.5\text{x}10^{11}$at 25 ns and $5\text{x}10^{11}$ at 50 ns bunch spacing appear feasible from the point of view of these heat loads.

Another heat-load contribution is from gas scattering onto the cold bore. Nuclear beam-gas scattering at a beam lifetime of τ~100 h (32 ntorr hydrogen pressure at room temperature) contributes a beam-screen heat-load equivalent of 0.15 W/m at nominal current; see e.g. [40]. This represents a rather small additional contribution, which does not change our above conclusion.

The heat load from electron cloud is obtained from simulations [42,43]. The most optimistic simulations consider a maximum secondary emission yield below 1.3, where beam-induced multipacting is largely absent, and where the remaining electron-induced heating is dominated by the accelerated primary photo-electrons.

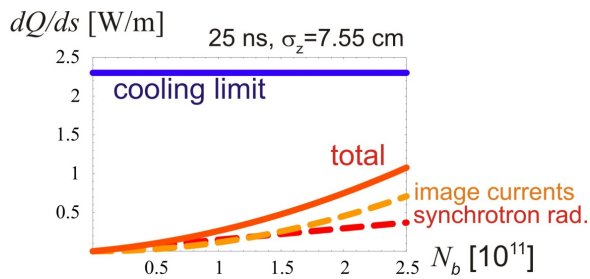

Figure 26: Heat load from synchrotron radiation and image currents, as well as their sum, as a function of bunch intensity, for a bunch spacing of 25 ns and an rms bunch length of 7.55 cm.

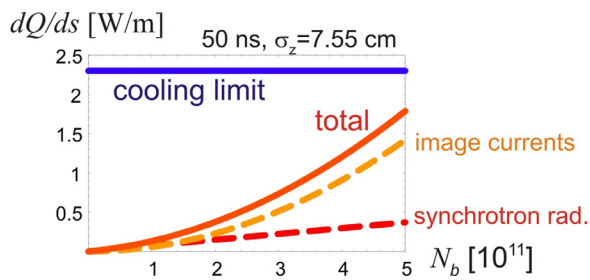

Figure 27: Heat load from synchrotron radiation and image currents, as well as their sum, as a function of bunch intensity, for a bunch spacing of 50 ns and an rms bunch length of 7.55 cm.

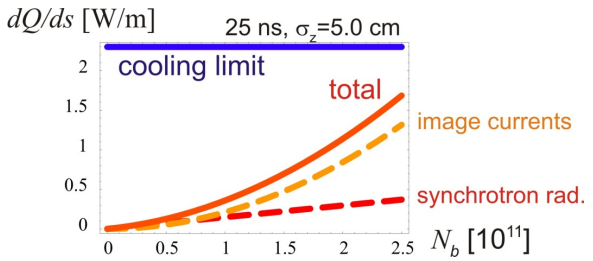

Figure 28: Heat load from synchrotron radiation and image currents, as well as their sum, as a function of bunch intensity, for a bunch spacing of 25 ns and an rms bunch length of 5.0 cm.

Figures 29 and 30 compare, for bunch-spacing values of 25 ns and 50 ns, respectively (and with different IP beta functions), the residual cooling capacity available and the simulated heat load from the electron cloud. Here, the residual (global) cooling capacity [without dedicated IR cryo-plants] was calculated by subtracting from the global limit the equivalent cooling power required for the interaction region (depending on the luminosity), and the computed heating from synchrotron radiation and image currents; by subtracting from the local limit only the latter two arc contributions; and then taking the minimum value of the remaining global and local cooling capacities so obtained.

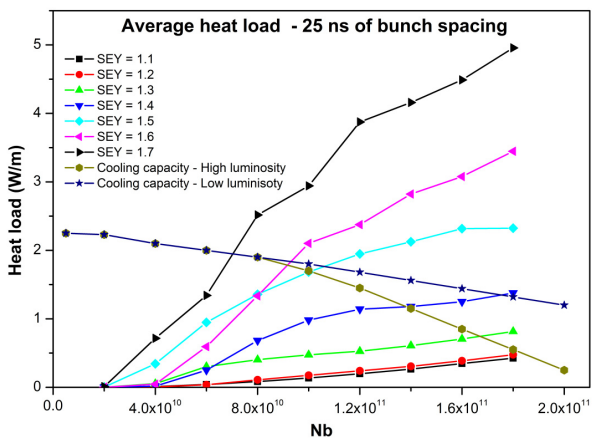

Figure 29: Residual cooling capacity for electron cloud per aperture and per meter at low and high luminosity at β^*=0.55 m (or with and without dedicated IR cryo plants) as a function of bunch intensity [37-39] together with the electron cloud heat load simulated for various values of the maximum secondary emission yield and 25-ns bunch spacing, with a Gaussian bunch profile [41,42].

Figures 29 and 30 demonstrate that in order to reach any decent bunch intensity at high luminosity (actually the first is a precondition for the latter), separate dedicated cryo plants are needed for the interaction regions. More specifically, Fig. 29 shows that for 25-ns bunch spacing, going above N_b=1.7x10^{11} protons per bunch at nominal β^* requires dedicated IR cryo plants; if such plants are installed the "hard" intensity limit becomes N_b~2.3x10^{11}. From Fig. 30, for 50-ns bunch spacing, dedicated IR cryo plants are required at bunch intensities above N_b=1.3x10^{11} with an upgraded β^*~0.25 m; again assuming a separate IR cooling, the hard limit on the bunch intensity is pushed to N_b~5x10^{11}.

In conclusion the additional electron cloud contribution to the beam-screen heat load is acceptable if $\delta_{max}\leq$1.2.

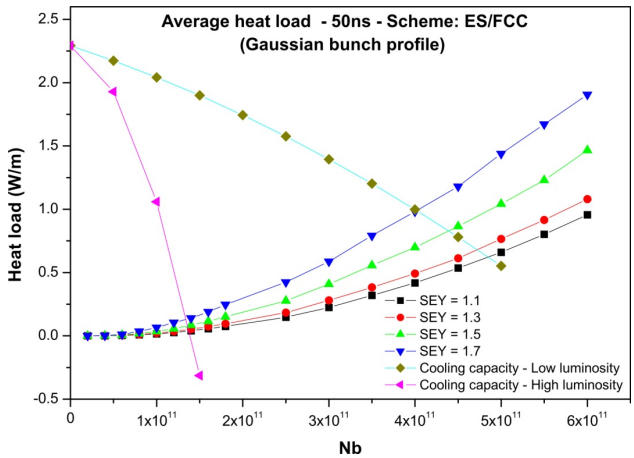

Figure 30: Residual cooling capacity for electron cloud per aperture and per meter at low and high luminosity (or with and without dedicated IR cryo plants) for a bunch spacing of 50 ns and β^*=0.25 m as a function of bunch intensity [37-39] together with the electron cloud heat load simulated for various values of the maximum secondary emission yield. A longitudinally Gaussian bunch shape is assumed [41,42].

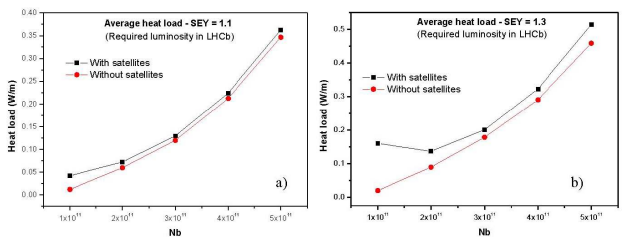

Figure 31: Simulated electron heat load as a function of main bunch intensity for 50 ns bunch spacing with (black) and without LHCb satellite bunches (red) for two different values of the maximum secondary emission yield (δ_{max}=1.1 – left, and δ_{max}=1.3 – right) [41,42]. In this simulation, the satellite bunch intensity has been varied as the inverse of the main-bunch intensity, namely as $N_{b,sat}$~1.1x10^{10} x 5x10^{11}/$N_{b,main}$, in order to obtain a constant target luminosity of about 2x10^{33} cm^{-2}s^{-1} in (S)LHCb.

Figure 31 presents simulated heat loads for the 50-ns bunch spacing of the standard 50-ns LPA scheme with and without additional dedicated LHCb satellite bunches interleaved at a distance of 25 ns from the main bunches [41,42] (see Fig. 32). Here, the satellite bunch intensity is decreased in inverse proportion to the main bunch intensity in order to provide a constant target luminosity in LHCb (determined by collisions between main bunches and satellites). Figure 31 illustrates that the heat load

including the "LHCb satellite" does not show a fully monotonic dependence on the main bunch intensity, which is consistent with earlier studies of other types of LHC satellite bunches [43,44], but that the additional smaller bunches only marginally increase the (low) 50-ns heat load.

We infer that the electron-cloud heat load would also be acceptable for 50-ns spacing plus "LHCb satellites".

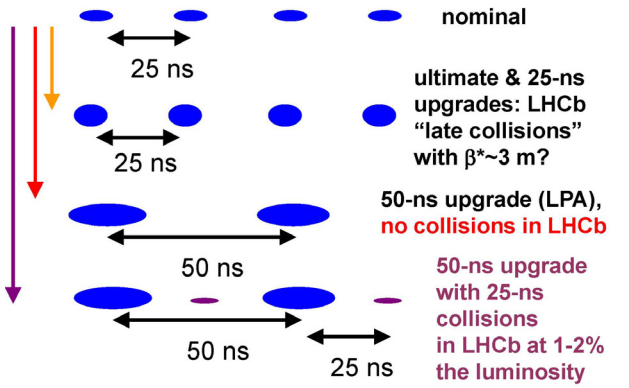

Figure 32: Bunch patterns for the LHC luminosity upgrade with and without collisions in (S)LHCb.

HL-LHC PARAMETER SETS

Tables 4-6 compile example parameter sets for the HLC-LHC. The three tables refer to $\beta_{x,y}^*$=15, $\beta_{x,y}^*$=30, and β_x^*=30 cm & β_y^*=7.5 cm (flat collision), respectively. The $\beta_{x,y}^*$ values considered in Tables 4 and 6 have been proposed and can be realized with the ATS scheme [11-13,25]. The $\beta_{x,y}^*$ values of Table 5 correspond to the minimum possible beta* available for the former SLHC Phase-I IR upgrade [45].

For each choice of IP beta functions, we consider alternative scenarios with crab cavities, higher-harmonic RF system (plus long-range beam-beam compensation), and 50-ns spacing (plus long-range beam-beam compensation) and, for each scenario, determine the bunch charge and total intensity required for delivering 300 fb^{-1} per year.

For the flat-beam cases the crossing angle has been taken to be 12.4σ^*', with σ^*' denoting the rms beam divergence at the IP in the plane of crossing. This crossing angle should be sufficient to confine the total tune footprint to a square with dimension 0.01x0.01 in tune units, e.g. see [10], possibly after adding a moderate long-range compensation. For the round-beam collision cases the crossing angle has been set to 8.5$\sigma_{x,y}^*$', requiring the presence of long-range beam-beam compensators.

The intrabeam scattering growth rates quoted in Tables 4-6 were obtained by scaling the IBS rates computed for the nominal LHC collision optics with bunch intensity. For the ATS optics the IBS growth rates would be further modified by the beta wave in the arcs, leading to a welcome increase in the longitudinal IBS rise time [11].

Table 4: Example HL-LHC parameters sets with $\beta_{x,y}^*$=15 cm and nominal emittance.

parameter	symbol	nom.	nom.*	HL crab	HL sb + lrc	HL 50+lrc
protons per bunch	N_b [10^{11}]	1.15	1.7	1.78	2.16	3.77
bunch spacing	Δt [ns]	25	50	25	25	50
beam current	I [A]	0.58	0.43	0.90	1.09	0.95
longitudinal profile		Gauss	Gauss	Gauss	Gauss	Gauss
rms bunch length	σ_z [cm]	7.55	7.55	7.55	5.0	7.55
beta* at IP1&5	β^* [m]	0.55	0.55	0.15	0.15	0.15
full crossing angle	θ_c [μrad]	285	285	(492-599)	492	492
Piwinski parameter	$\phi=\theta_c\sigma_z/(2*\sigma_x^*)$	0.65	0.65	0.0	1.42	2.13
tune shift	ΔQ_{tot}	0.009	0.0136	0.011	0.008	0.010
virtual peak luminosity	L [10^{34} cm^{-2}s^{-1}]	1	1.1	10.6	9.0	10.1
events per #ing		19	40	95	95	189
effective lifetime	τ_{eff} [h]	44.9	30	13.9	16.8	14.7
run or level time	$t_{run,level}$ [h]	15.2	12.2	4.33	4.26	4.35
e-c heat SEY=1.2	P [W/m]	0.2	0.1	0.4	0.6	0.3
SR+IC heat 4.6-20 K	P_{SR+IC} [W/m]	0.32	0.30	0.63	1.30	1.09
IBS ε rise time (z, x)	$\tau_{IBS,z/x}$ [h]	59, 102	40, 69	38, 66	8, 33	18, 31
annual luminosity	L_{int}[fb^{-1}]	57	58	300	300	300

Table 5: Example HL-LHC parameters sets with $\beta_{x,y}^*$=30 cm and nominal emittance.

parameter	symbol	nom.	nom.*	HL crab	HL sb + lrc	HL 50+lrc
protons per bunch	N_b [10^{11}]	1.15	1.7	2.28	2.47	4.06
bunch spacing	Δt [ns]	25	50	25	25	50
beam current	I [A]	0.58	0.43	1.15	1.25	1.03
longitudinal profile		Gauss	Gauss	Gauss	Gauss	Gauss
rms bunch length	σ_z [cm]	7.55	7.55	7.55	5.0	7.55
beta* at IP1&5	β^* [m]	0.55	0.55	0.30	0.30	0.30
full crossing angle	θ_c [μrad]	285	285	(348-447)	348	348
Piwinski parameter	$\phi=\theta_c\sigma_z/(2*\sigma_x^*)$	0.65	0.65	0.0	0.71	1.06
tune shift	ΔQ_{tot}	0.009	0.0136	0.0145	0.0128	0.0177
virtual peak luminosity	L [10^{34} cm^{-2}s^{-1}]	1	1.1	8.66	8.29	9.41
events per #ing		19	40	95	95	189
effective lifetime	τ_{eff} [h]	44.9	30	17.8	19.3	15.8
run or level time	$t_{run,level}$ [h]	15.2	12.2	4.27	4.31	4.29
e-c heat SEY=1.2	P [W/m]	0.2	0.1	0.6	0.7	0.3
SR+IC heat 4.6-20 K	P_{SR+IC} [W/m]	0.32	0.30	0.93	1.65	1.24
IBS ε rise time (z, x)	$\tau_{IBS,z/x}$ [h]	59, 102	40, 69	30, 52	7, 29	17, 29
annual luminosity	L_{int}[fb^{-1}]	57	58	300	300	300

Table 6: Example HL-LHC parameters sets for flat beams with β_x^*=30 cm, β_y^*=7.5 cm, and nominal emittance.

parameter	symbol	nom.	HL crab flat	HL sb+lrc flat	HL 50+lrc flat
protons per bunch	N_b [10^{11}]	1.15	1.78	2.02	3.45
bunch spacing	Δt [ns]	25	25	25	50
beam current	I [A]	0.58	0.90	1.02	0.87
longitudinal profile		Gauss	Gauss	Gauss	Gauss
rms bunch length	σ_z [cm]	7.55	7.55	5.0	7.55
beta* at IP1&5	$\beta_{x,y}^*$ [m]	0.55	0.30, 0.075	0.30, 0.075	0.30, 0.075
full crossing angle	θ_c [μrad]	285	(507-618)	507	507
Piwinski parameter	$\phi=\theta_c\sigma_z/(2*\sigma_x^*)$	0.65	0.0	1.03	1.55
tune shift	ΔQ_{tot}	0.009	0.011	0.0079	0.0098
virtual peak luminosity	L [10^{34} cm^{-2}s^{-1}]	1	10.6	9.5	10.8
events per #ing		19	95	95	189
effective lifetime	τ_{eff} [h]	44.9	13.9	15.8	13.5
run or level time	$t_{run,level}$ [h]	15.2	4.33	4.30	4.28
e-c heat SEY=1.2	P [W/m]	0.2	0.4	0.6	0.3
SR+IC heat 4.6-20 K	P_{SR+IC} [W/m]	0.32	0.63	1.16	0.94
IBS ε rise time (z, x)	$\tau_{IBS,z/x}$ [h]	59, 102	38, 66	9, 35	19, 34
annual luminosity	L_{int}[fb^{-1}]	57	300	300	300

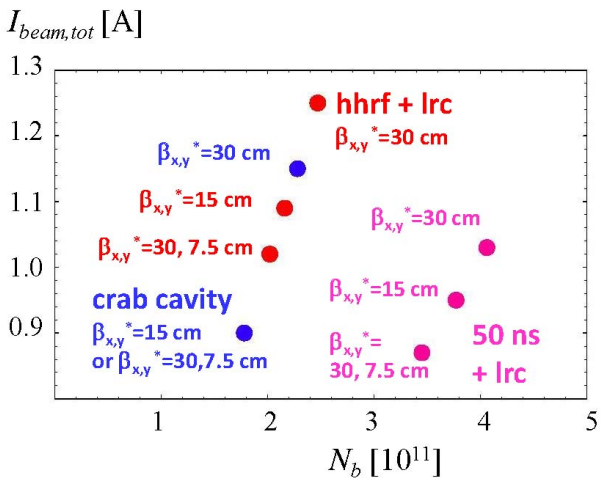

Figure 33: Total beam current and proton bunch intensity required for the different upgrade scenarios of Tables 4-6. "hhrf" refers to the higher harmonic RF system, "lrc" to long-range compensation.

Figure 33 graphically presents the results in the total-intensity/bunch-intensity plane. It is evident that 50-ns scenarios allow for larger IP beta functions and/or reduced total beam current at the same integrated luminosity, and that a flat beam-optics may be preferred compared with round beams. For 25-ns bunch spacing, the crab-cavity upgrade scenario is most appealing.

The luminosity time evolution is almost the same for all scenarios. Figure 34 displays a typical HL-LHC luminosity evolution over 24 h.

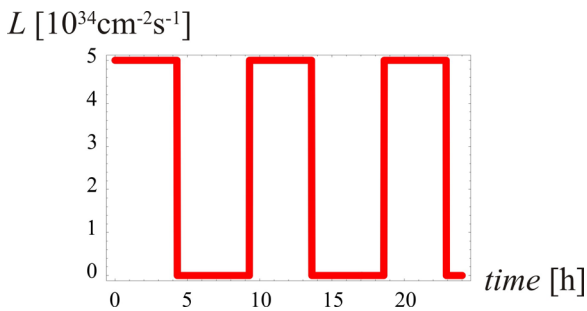

Figure 34: Luminosity evolution during a "typical day" at the HL-LHC. It is similar for all scenarios considered.

PRELIMINARY CONCLUSIONS

The HL-LHC parameter space is well defined. In order to achieve 300 fb^{-1} per year the following ingredients are required:

- about 1 A beam current (+/- 10%);
- potential peak luminosity 10^{35} cm^{-2}s^{-1};
- run time of 4.3 h, assuming 5-h turnaround time;
- β* between 7.5 and about 30 cm, possibly flat.

A high(er) beam intensity helps in every regard. Both 50-ns and 25-ns scenarios are possible, with a preference for the former. Aiming at 200 fb^{-1} per year only would relax the intensity demand. The beam-beam limit (at a value of 0.02 or above) is no longer a serious constraint.

Several alternative scenarios for 300 fb^{-1} / year have been constructed using

- crab cavities;
- higher harmonic RF (shorter bunches) and long-range beam-beam compensation;
- 50-ns bunch spacing, large Piwinski angle, and long-range beam-beam compensation;

for each case considering the impact of different round or flat IP beta functions. Decreasing β* from 30 to 15 cm is equivalent to 10-30% beam current increase (scenario-dependent).

Scenarios with 50-ns spacing are attractive, as are 25-ns scenarios with crab cavities.

PROPOSED ROADMAP & BRANCHING POINTS

Starting in 2011, LHC MDs for HL-LHC should address the following points

- ATS optics ingredients (beta wave, phase changes);
- long-range beam-beam limits;
- effect of crossing angle on the head-on beam-beam limit;
- limits related to electron cloud;
- "flat beam" optics, e.g. $\beta_x^*/\beta_y^* \sim 2$, with an effective gain in aperture of $\Delta n_1 \sim 1\sigma$ [8]; and
- effect of the crossing planes (H-V, V-V, H-H).

It is suggested to install prototype long-range beam-beam compensators in the LHC during the first long shutdown (2013), to develop & prototype compact crab cavity (2011-16) for beam test in (SPS+) LHC (2017), and to develop & install an LHC 800-MHz RF system (2016?).

In the coming years, LHC operational experience with electron-cloud and long-range beam-beam effects at 25-ns and 50-ns bunch spacing, results of ATS optics machine studies, and progress on crab-cavity development & crab-cavity beam testing will together determine the HL-LHC upgrade path to be taken.

ACKNOWLEDGEMENTS

I would like to thank many colleagues and friends, who have - over the last decade - contributed ideas on the LHC upgrade, including R. Assmann, R. Bailey, C. Bhat, O. Brüning, R. Calaga, H. Damerau, R. De Maria, D. Denegri, O. Dominguez, U. Dorda, L. Evans, S. Fartoukh, R. Garoby, M. Giovannozzi, B. Goddard, N. Hessey, B. Holzer, B. Jeanneret, E. Jensen, J.-P. Koutchouk, H. Maury Cuna, S. Myers, J. Nash, M. Nessi, K. Ohmi, R. Ostojic, Y. Papaphilippou, L. Rossi, F. Ruggiero, G. Rumolo, W. Scandale, D. Schulte, E. Shaposhnikova, G. Sterbini, K. Takayama, L. Tavian, T. Taylor, E. Todesco, R. Tomas and E. Tsesmelis.

APPENDIX: LUMINOSITY DECAY AND LIFETIME

For the upgraded LHC a fast decay of beam intensity and luminosity is expected (with a typical time scale of a few hours), which is dominated by proton burn off in proton-proton collision. Contributions from intrabeam scattering and from gas scattering can be considered negligible in comparison. Under these conditions, the luminosity decay will not be exponential, but purely algebraic, and of the form [31]

$$L(t) = \frac{\hat{L}}{\left(1 + t/\tau_{eff}\right)^2} \qquad (4)$$

where τ_{eff} denotes the effective initial beam lifetime

$$\tau_{eff} = \frac{N_b n_b}{n_{IP} \hat{L} \sigma_{tot}} \qquad (5)$$

and we recognize the number of protons per bunch N_b, the number of bunches per beam n_b, the number of IPs, the initial peak luminosity $\hat{L}$ and the total interaction cross section σ_{tot}.

The beam and luminosity lifetimes are proportional to the total beam intensity and inversely proportional to the luminosity. An LHC luminosity upgrade implies shorter luminosity lifetimes unless the beam intensity is increased simultaneously. Or, in other words, for a given luminosity, the luminosity lifetime depends only on the total beam current.

Table 7 compiles helpful expressions describing the time evolution of luminosity and beam current, the optimum run time, and time-averaged luminosity without and with luminosity levelling, and for levelling of the beam-beam tune shift.

Table 7: Analytical expressions for the time evolution of luminosity and beam current, for the optimum run time, and for the average luminosity, with and without levelling, and considering two different levelling schemes. "T_{ta}" denotes the average "turnaround time", that is the time from the end of a "physics" fill to the start of the next "physics" period.

	w/o leveling	L=const	ΔQ_{bb}=const
luminosity evolution	$L(t) = \frac{\hat{L}}{\left(1 + t/\tau_{eff}\right)^2}$	$L = L_0 \approx const$	$L(t) = \hat{L}\exp\left(-t/\tau_{eff}\right)$
beam current evolution	$N(t) = \frac{N_0}{\left(1 + t/\tau_{eff}\right)}$	$N = N_0 - \frac{N_0}{\tau_{eff}} t$	$N(t) = N(0)\exp\left(-t/\tau_{eff}\right)$
optimum run time	$T_{run} = \sqrt{\tau_{eff} T_{ta}}$	$T_{run} = \frac{\Delta N_{\max} \tau_{eff}}{N_0}$	$T_{run} = \tau_{eff} \min\left[\ln\left(\sqrt{1+\phi_{piw}(0)^2}\right), \ln\left(\left(T_{ta} + T_{run} + \tau_{eff}\right)/\tau_{eff}\right)\right]$
average luminosity	$L_{ave} = \hat{L}\frac{\tau_{eff}}{\left(\tau_{eff}^{1/2} + T_{ta}^{1/2}\right)^2}$	$L_{ave} = \frac{L_0}{1 + \frac{L_0 \sigma_{tot} n_{IP}}{\Delta N_{\max} n_b} T_{ta}}$	$L_{ave} = \frac{\tau_{eff}}{T_{ta} + T_{run}}\left(1 - e^{-T_{run}/\tau_{eff}}\right)$

REFERENCES

[1] O. Brüning et al., "LHC Luminosity and Energy Upgrade: A Feasibility Study," CERN-LHC-Project-Report-626 (2002)

[2] CARE-HHH network, web site http://cern.ch/care-hhh .

[3] Proceedings of the 1st CARE-HHH-APD Workshop on *Beam Dynamics in Future Hadron Colliders and Rapidly Cycling High-Intensity Synchrotrons* – 'HHH 2004,' CERN, Geneva, November 2004, edited by F. Ruggiero, W. Scandale, F. Zimmermann, CERN Yellow Report 2005-006.

[4] Proceedings of the 3rd CARE-HHH-APD Workshop: *Towards a Roadmap for the Upgrade of the LHC and GSI Accelerator Complex* – 'LHC-LUMI-06,' Valencia, Spain, October 2006, edited by W. Scandale, T. Taylor, F. Zimmermann, CERN Yellow Report 2007-002

[5] Proceedings of the CARE-HHH-APD Workshop on Finalizing the Roadmap for the Upgrade of the CERN and GSI Accelerator Complex – 'BEAM'07,' BEAM'07, CERN, Geneva, October 2007, edited by W. Scandale, and F. Zimmermann, CERN Yellow Report 2008-005.

[6] Proceedings of the Final CARE-HHH Workshop on *Scenarios for the LHC Upgrade and FAIR* – 'HHH-2008,' Chavannes-de-Bogis, November 2008, edited by W. Scandale, and F. Zimmermann, CERN Yellow Report 2009-004.

[7] EuCARD-AccNet network, web site http://accnet.lal.in2p3.fr/

[8] F. Zimmermann, Parameter Space Beyond 10^{34}," in Proc. Chamonix 2010 Workshop on LHC Performance, CERN-ATS-2010-026 (2010)

[8] S. Fartoukh, "Flat Beam Optics," 19th Meeting of the LHC Machine Advisory Committee, 16 June 2006.

[9] O. Brüning, "Do we really need the LHC luminosity upgrade? Or, which performance can we get without an upgrade?" in Proc. Chamonix 2011 Workshop on LHC Performance (these proceedings) (2011)

[10] J.-P. Koutchouk, "Luminosity optimization and leveling," Proc. Chamonix 2010 Workshop on LHC Performance (edited by C. Carli), CERN-ATS-2010-026 (2010).

[11] S. Fartoukh, "Breaching the Phase I optics limitations for the HL-LHC," in Proc. Chamonix 2011 Workshop on LHC Performance (these proceedings) (2011).

[12] S. Fartoukh, "Towards the LHC Upgrade using the LHC Well-Characterized Technology," sLHC-PROJECT-Report-0049 (2010).

[13] R. De Maria, S. Fartoukh, "SLHCV3.0: Layout, Optics and Long Term Stability," sLHC-PROJECT-Report-0050 (2010).

[14] S.D. Holmes (ed.), "Tevatron Run-II Handbook," FERMILAB-TM-2484-1998, Section 6.2 (1998).

[15] D. Brandt, "Review of the LHC Ion Programme," LHC Project Report 450 (2000).

[16] F. Zimmermann, W. Scandale, "Two Scenarios for the LHC Luminosity Upgrade," CERN Joint PAF/POFPA meeting on 13.02.2007.
[17] G. Sterbini, J.-P. Koutchouk, "A Luminosity Leveling Method for LHC Luminosity Upgrade using an Early Separation Scheme," LHC-Project-Note-403 (2007), issued 21.05.2007
[18] W. Scandale, F. Zimmermann, "Scenarios for sLHC and vLHC," 18th Hadron Collider Physics Symposium 2007 (HCP 2007) 20-26 May 2007, La Biodola, Isola d'Elba, Italy. Published in Nucl. Phys. Proc. Suppl. 177-178: 207-211 (2008).
[19] Review of Particle Physics. Particle Data Group (C. Amsler et al.). Published in Phys. Lett. B667:1, 2008.
[20] M. Ferro-Luzzi, "LHC Operation – as viewed from the Experiments," in Proc. Chamonix 2011 Workshop on LHC Performance (these proceedings) (2011)
[21] W. Venturini Delsolaro, "Operational Efficiency," LHC Beam Operation Workshop Evian, December 2010
[22] J. Seeman, private communication, 31.01.2011
[23] V. Shiltsev, private communication, 31.01.2011
[24] W. Fischer, private communication, 31.01.2011
[25] R. De Maria, S. Fartoukh, "Upgrade Optics with Crab Cavities," at Fourth LHC Crab Cavity Workshop "LHC-CC'10," CERN, Geneva, 15-17.12.2010; see [27] (2010).
[26] J. Tuckmantel, "The Ultimate Beam in the LHC 400 MHz RF System," CERN-ATS-Note-2010-038 TECH (2010).
[27] Fourth LHC Crab Cavity Workshop "LHC-CC'10," CERN, Geneva, 15-17.12.2010, indico web site: http://indico.cern.ch/conferenceOtherViews.py?view=standard&confId=100672 ; workshop summary edited by R. Calaga, F. Zimmermann to be published.
[28] D. Shatilov, E. Levichev, E. Simonov, and M. Zobov, "Application of frequency map analysis to beam-beam effects study in crab waist collision scheme," Phys. Rev. ST Accel. Beams 14, 014001 (2011).
[29] K. Ohmi, O. Dominguez, F. Zimmermann, "Beam-Beam Studies for the High-Energy LHC," Proc. EuCARD-AccNet HE-LHC'10 Workshop, Malta, 14-16 October 2010; proceedings to be published as CERN Yellow Report.
[30] J.-P. Koutchouk, "Principle of a Correction of the Long-Range Beam-Beam Effect in LHC using Electromagnetic Lenses," LHC-PROJECT-NOTE-223 (2010)
[31] U. Dorda et al, «Wire excitation experiments in the CERN SPS, » Proc. EPAC'08 Genoa, CERN-LHC-PROJECT-Report-1102 (2008); F. Zimmermann et al, "Experiments on LHC Long-Range Beam-Beam Compensation and Crossing Schemes at the CERN SPS in 2004," PAC"05 Knoxville, LHC-Project-Report-844 (2005); J.-P. Koutchouk et al, "Experiments on LHC Long-Range Beam-Beam Compensation in the CERN SPS," EPAC'04 Lucerne, LHC-Project-Report-777 (2004).
[32] W. Fischer et al., "Long-range and Head-on Beam-Beam Compensation Studies in RHIC with Lessons for the LHC" Proc. CARE HHH-2008 Workshop, 25-25.11.2008, Chavannes-de-Bogis; CERN-2009-004 (2009); W. Fischer et al, "Experiments with a DC wire in RHIC," PAC'07 Albuquerque, SLAC-PUB-12791 (2007).
[33] Y. Papaphilippou, F. Zimmermann, "Weak-Strong Beam-Beam Simulations for the Large Hadron Collider," Phys.Rev.ST - AB 2:104001, (1999).
[34] P. Raimondi, M. Zobov : "Tune Shift in Beam-Beam Collisions with a Crossing Angle," DAFNE-TECHNICAL-NOTE-G-58 (2003).
[35] T. Linnecar and E. Shaposhnikova, "An RF System for Landau Damping in the LHC," LHC Project Note 394 (2007).
[36] E. Shaposhnikova, private communication (2010).
[37] Discussions with L. Tavian and B. Jeanneret, early in 2005
[38] F. Zimmermann, "Electron Cloud Update," 17th Meeting of the LHC Machine Advisory Committee, 10 June 2005
[39] L. Tavian, "Cryogenic Limits," presentation at CARE-HHH LUMI'06 workshop, Valencia, Spain; http://care-hhh.web.cern.ch/CARE-HHH/LUMI-06/
[40] B. Jeanneret, F. Zimmermann, "What is an Acceptable Vacuum Pressure in the LHC Arcs?," Proc. 1st CARE-HHH-APD Workshop on Beam Dynamics in Future Hadron Colliders and Rapidly Cycling High-Intensity Synchrotrons "HHH-2004", CERN, Geneva, Switzerland, 8 - 11 November 2004, CERN Yellow Report CERN-2005-006 (2005).
[41] H. Maury Cuna, "Study of the Heat Load due to the Electron Cloud in the LHC and in Higher-Luminosity LHC Extensions," (in Spanish), Master Thesis U. Merida (and shortened English version), August 2009; available at http://ab-abp-rlc.web.cern.ch/ab-abp-rlc-ecloud/
[42] H. Maury, J. Guillermo, F. Zimmermann, "Simulations of Electron-Cloud Heat Load for the Cold Arcs of the LHC and Its High-Luminosity Upgrade Scenarios," submitted to PRST-AB (2010).
[43] F. Ruggiero, X. Zhang, "Collective instabilities in the LHC: Electron cloud and satellite bunches," Workshop on instabilities of high intensity hadron beams in rings. AIP Conference Proceedings, Volume 496, pp. 40-48 (1999).
[44] F. Zimmermann, "Electron-Cloud Simulations for SPS and LHC," Proceedings of LEP and LHC Performance Workshop Chamonix X, January 2000, CERN-SL-2000-007 DI.
[45] S. Fartoukh, "Optics Challenges and Solutions for the LHC Insertions Upgrade Phase I," in Proc. Chamonix 2010 Workshop on LHC Performance, CERN-ATS-2010-026 (2010).